Purification and characterization of microRNAs within middle ear fluid exosomes: implication in otitis media pathophysiology

Stéphanie Val[1], Stephanie Jeong[1], Marian Poley[1], Anna, Krueger[1], Gustavo Nino[2,3], Kristy Brown[2] and Diego Preciado[1,4]

BACKGROUND: Otitis media (OM) is characterized by acute infection progressing to chronic middle ear effusion (MEE). Extracellular secretion of microRNAs (miRNAs) in exosomes is a newly discovered mechanism for cells exerting distant cell genetic regulation. Whether MEE contains exosomes with specific miRNAs is unknown. This study aimed to purify and characterize the exosomal and miRNA content of MEE.

METHOD: MEEs were subjected to Exoquick exosomal purification and EXOCET exosomal quantification. Extracted vesicles were analyzed by dynamic light scattering (DLS), transmission electron microscopy (TEM), and immunoblotting of HSP-70. NanoString hybridization was performed to profile miRNAs. Exosomal protein content was profiled by Liquid chromatography tandem mass spectrometry (LC-MS/MS).

RESULTS: EXOCET assays showed presence of exosomes (0–0.5×10^7/ml) in MEEs. DLS confirmed exosomal size between 10 and 200 nm. Western blot analysis showed presence of HSP-70. Twenty-nine miRNAs were found to be unique to MEEs. The most abundant miRNA was miR-223, a miRNA typically secreted by neutrophils. Proteomics demonstrated typical neutrophil markers as well as common innate immune molecules.

CONCLUSION: To our knowledge, this the first report demonstrating the presence of exosomes transporting miRNAs in MEEs. These findings open a broad and novel area of research in OM pathophysiology as driven by miRNA cell communication.

Otitis media (OM) is one of the most common conditions of early childhood accounting for a very high proportion of all pediatric office visits and surgeries annually (1,2) at a national health care cost estimated to be greater than $1 billion (3,4). Chronic otitis media (COM) typically results as a long term sequelae of recurrent acute middle ear infections, and is characterized by persistence of middle ear effusion (MEE), most frequently mucoid (5–7). This viscous middle ear effusion has been shown to be primarily composed of innate immunity mediators derived from neutrophils (8,9), such as neutrophil extracellular traps (NETs) (10,11); along with secretory mucin glycoproteins, predominantly MUC5B (12).

The progression of OM from acute OM (AOM) to COM, has long been shown to be in part under the influence of proinflammatory mediators, specifically through bacterial activation of epithelial proinflammatory pathways (reviewed in (13)), that drive middle ear epithelial remodeling into a pseudostratified epithelium in COM able to potently produce mucins (14–16). Recently, exosomes have been described as important mediators of intercellular communication. Exosomes are actively shed endocytic vesicles that contain and transport functional mRNAs, microRNAs (miRNAs), and proteins between cells (17,18). MiRNAs are small, ~20–22 nucleotide, noncoding RNAs that post-transcriptionally regulate gene expression by binding to the 3′-untranslated region of target mRNAs (19). Indeed, exosomal derived miRNAs have been shown to stringently influence either positive or negative gene effects on proinflammatory signaling in distant cells (20,21), as well as being implicated in many diseases such as cancer, and cardiac disease among others (22). Extracellular miRNAs have been proposed as relevant biomarkers for disease detection (23). In OM models, bacterial products have been shown to drive differential expression of miRNAs in human middle ear epithelial cells (HMEECs) *in vitro* (24). However, to our knowledge, no study to date has isolated and characterized exosomal derived microRNAs from human COM effusion samples. Importantly, in parallel respiratory diseases, such as chronic lung diseases, epithelial derived exosomes have been shown to drive local inflammation through significant macrophage and neutrophil activation (25). Further, these events serve as crucial mediators of acute lung injury (26). Whether similar processes could be going on in OM pathophysiology remains mostly unexplored and is the impetus for our work, but neutrophilic inflammation appears to be key in OM disease development (9).

For this study, we hypothesized that middle ear effusions would contain exosomes that harbor mediators capable of influencing the neutrophilic inflammation typical of COM.

[1]Sheikh Zayed Center for Pediatric Surgical Innovation, Children's National Health System, Washington, DC; [2]Center for Genetic Medicine Research, Children's National Health System, Washington, DC; [3]Division of Pediatric Pulmonology, Children's National Health System, Washington, DC; [4]Division of Pediatric Otolaryngology, Children's National Health System, Washington, DC. Correspondence: Diego Preciado (dpreciad@cnmc.org)

Received 3 October 2016; accepted 27 December 2016; advance online publication 5 April 2017. doi:10.1038/pr.2017.25

METHODS

Sample Collection and Preparation

The Institutional Review Board Committee of Children's National Health System approved this study. After obtaining written informed consent from the legal guardian, effusions from children aged 6–36 mo with COM, undergoing myringotomy with tube placement irrespective of race/ethnicity/gender were collected. For sample analysis, effusions from each ear were pooled into one sample per patient. Exclusion criteria included: cleft palate or other craniofacial dysmorphic syndromes, immunosuppressive states or conditions, cystic fibrosis, immotile cilia syndrome, or prior history of skull base radiation therapy or skull base malignancy. A total of 23 samples of MEE from pediatric patients with COM were collected fresh, aliquoted, and if not immediately used for experiments, frozen at −80 °C. Subsets of MEE were used for exosome isolation and characterization depending on extracted RNA amount and sample volume.

Exosome Isolation

Exosomes were isolated with the Exoquick-TC kit (System Biosciences, Mountain View, CA). Briefly, samples were diluted in 1 ml of PBS and 200 µl of each sample was centrifuged at 1,500 g for 15 min to remove cells and cell debris. The supernatant was mixed with 40 µl of Exoquick buffer and incubated overnight at 4 °C. The day after, the tubes were centrifuged at 1,500 g for 30 min and the exosome pellet was reconstituted in 100 µl of PBS 1×, and stored at −80 °C until further analysis.

Exosome Quantification Assay: EXOCET Assay

The EXOCET assay (System Biosciences) was used to quantify exosomes isolated from MEEs, according to the manufacturer recommendations. Briefly, the EXOCET assay quantifies the activity of the acetyl-CoA acetylcholinesterase known to be within exosomes, through colorimetric change. Ten microliters of exosomes in PBS were diluted in 100 µl of exosome lysis buffer and incubated 5 min at 37 °C to liberate exosome proteins. The samples were centrifuged at 1,500 g for 5 min to remove debris. Fifty microliters of this preparation were incubated with the enzyme substrate in a 96-well plate. Four hours after the plate was read at 405 nm to quantify the production of the enzyme product relative to an internal control standard.

Western Blot Analysis of Exosome Markers

A previously described protocol was used for western blotting (27). Ten microliters of isolated vesicles from each sample were mixed with 20 µl of RIPA buffer (SigmaAldrich, St. Louis, MO) and incubated at room temperature to liberate exosome proteins. They were mixed with Laemmli buffer and placed at 95 °C for 10 min. Samples were then separated by electrophoresis on NuPAGE Novex 4–12% Bis-Tris gels (Life Technologies, Carlsbad, CA). The molecular weight marker Kaleidoscope was used as a standard (Bio-Rad, Hercules, CA). Proteins were then transferred to a nitrocellulose membrane (Life Technologies). Membranes were blocked with 5% non-fat dry milk in PBS with 0.05% Tween-20 (PBST), and incubated with the rabbit HSP70 antibody (System Biosciences) at 1:5,000 and rabbit CD63 antibody (Systems Biosciences) at 1:5,000. A secondary antibody anti-rabbit at 1:10,000 coupled to horseradish peroxidase (System Biosciences). Detection was performed with a SuperSignal West Dura Extended Duration Substrate kit (Pierce, Rockland, IL) according to the manufacturer's instructions.

Determination of Exosome Size by Dynamic Light Scattering

The size of exosomes was evaluated using a Zetasizer Nano ZS system (Malvern Instruments, Malvern, UK) using the DLS technique analyzing the velocity distribution of particle movement by measuring the dynamic fluctuations of scattered light intensity at a fixed angle caused by the Brownian motion of the particle. The particle's hydrodynamic radius, or considered diameter, is then calculated with the Stokes–Einstein equation (see www.malvern.com). After exosome isolation with the Exoquick-TC, the pellet was reconstituted in 100 µl of PBS 1×. Ten microliters of purified exosomes were diluted in 990 µl of filtered PBS 1× and vortexed for 1 min. The whole volume was quickly put in a disposable cuvette for size measurements to avoid aggregation of the exosomes. Three independent measurements were performed for each sample and averaged by the software for the analysis.

Transmission Electron Microscopy of Isolated Exosomes

After exosome isolation with the Exoquick-TC, the pellet was reconstituted in 100 µl of PBS 1× filtered through a 0.2 µm membrane and used soon thereafter, so as to not damage the structure of the exosomes. Ten microliters of a 1/20 dilution of purified exosomes were then plated onto carbin coated formvar grids (Electron Microscopy Sciences, Hatfield, PA), fixed with a solution of 2% glutaraldehyde 0.1M cacodylate, stained with 4% aqueous uranul acetate, and imaged with a FEI Talos F200X Transmission Electron Microscope (Brno, Czech Republic) at 80 KV.

miRNA Isolation and Analysis

The miRNAs were isolated with the SeraMir columns (System Biosciences) using the protocol recommended by the supplier. The quality of the miRNA was then evaluated using the Agilent Small RNA kit and the Agilent RNA 6000 Nano Kit for the total RNA (Agilent Technologies, Santa Clara, CA).

Nanostring Identification of miRNAs

The global microRNA profile was obtained using NanoString human microarrays (human V2 miRNA array >800 probes, Nanostring Technologies, Seattle, WA). To account for differences in hybridization and purification, data were normalized to the average counts for all control spikes in each sample using proprietary bioinformatics software (nSolver Analysis Software 2.5, Nanostring Technologies, Seattle, WA). Briefly, we calculated a background level of expression for each sample using the mean level of the negative controls plus 2 SD of the mean. MiRNAs expressing less than 2 SD from the mean were set to 0 expression. Those miRNAs that were considered non-zero expression, were normalized using a scaling factor based on the top 100 expressing miRNAs across all samples. For each sample, the average of the geometric means of the top 100 expressing miRNAs across all samples was divided by the geometric mean of each sample (http://www.NanoString.com/media/pdf/MAN_nCounter_Gene_Expression_Data_Analysis_Guidelines.pdf).

Validation of miRNAs by PCR

miRNAs of interest were validated by polymerase chain reaction of the isolated exosomal RNA. After the isolation of miRNAs with the SeraMir kit, 100 ng of total miRNA was used for the reverse transcription, performed with the miScript Reverse Transcriptase kit (Qiagen, Redwood City, CA) according to the manufacturer's recommendations. The real-time PCR was then performed on the cDNA generated, with the QuantiTect SYBR Green PCR kit (Qiagen). The kit uses a miRNA universal primer in addition with primers targeting miRNAs of interest. The primers used were: Hs_miR-223_1 miScript Primer Assay, Hs_miR-16_2 miScript Primer Assay, and Hs_miR-320e_1 miScript Primer Assay. In addition, control and normalization gene/miRNA were provided by the kit: Human RNU6B (RNU6-2) miScript Primer Assay and Human miR-15a miScript Primer Assay. Those three miRNAs were chosen for validation because we intended to validate three abundant miRNAs for which we had primers readily available. Notably, 223-3p, 320e, and 16-2p have all been implicated in neutrophilia, inflammation, and programmed cell death (28,29).

Preparation of Exosome Proteins for Mass Spectrometry Analysis

Twenty microliters of isolated vesicles were mixed with 80 µl of RIPA buffer (Sigma Aldrich) and the total protein concentration was determined using Bicinchoninic Acid Microtiter Plate Assays (Pierce).

The detergent was first removed from the samples (50 µl of protein) with Pierce Detergent Removal Spin Column (ThermoScientific, Waltham, MA). The proteins were then digested into peptides using the SMART digest kit (ThermoScientific) and fractionated with the Pierce High pH Reversed–Phase Peptide Fractionation columns (ThermoScientific). Eight tubes per sample were generated, using different concentrations of acetonitrile. Extracted peptides were then completely dried in a SpeedVac (ThermoScientific).

Mass Spectrometry and Protein Identification

MS was carried out as previously described (12,30,31). Briefly, dried peptides were resuspended in trifluoroacetic acid (TFA) and 6 µl was injected and loaded onto a C18 trap column. The sample was subsequently separated by a C18 reverse-phase column. The mobile phases

consisted of water with 0.1% formic acid (A) and 90% acetonitrile with 0.1% formic acid (B). A 65-min linear gradient from 5 to 60% B was used. Eluted peptides were introduced into the mass spectrometer via a 10-μm silica tip (New Objective, Ringoes, NJ) adapted to a nano-electrospray source (Thermo Scientific). The spray voltage was set at 1.2 kV and the heated capillary at 200 °C. The linear trap quadrupole (LTQ) mass spectrometer (ThermoScientific) was operated in data-dependent mode with dynamic exclusion in which one cycle of experiments consisted of a full-MS (300–2,000 m/z) survey scan and five subsequent MS/MS scans of the most intense peaks. Pathways enriched with the proteins were generated by Ingenuity Pathways Analysis (IPA, version 8.5, Ingenuity Systems, Redwood City, CA). Relative protein amounts for each sample compared to the blood control were done by using peptide counts as a measurement of "amount" for each identified protein.

Ingenuity Pathway Analysis

The average counts of the 17 specific MEE miRNAs were entered in IPA. Predicted targets were generated from this dataset. To do so, the miRNA Target Filter analysis tool was used, focusing on the targets experimentally verified and highly conserved predicted targets. The list of mRNAs generated was then analyzed with the Core analysis tool and pathways with a P value < 0.01 were considered. Results shows relevant OM pathways activated as predicted by the dataset analysis.

RESULTS

Patient Characteristics and Sample Processing

Samples were collected from 23 COM patients undergoing myringotomy at Children's National Health System in Washington, DC. Mean age of patients was 25.3 mo. All subjects had presented with effusions lasting greater than 3 mo and had conductive hearing loss of 20–40 dB at 500 Hz. Importantly, given limitations in sample and extracted RNA volume, not every single middle ear fluid specimen could be profiled by each experimental technique. All 23 samples collected underwent exosome extraction through the Exoquick assay, of these 16 also had exosomal quantification through Exocet, and 6 were used directly for miRNA profiling through Nanostring analysis. The remaining sample was used for proteomics. Of the 16 samples used for Exocet quanitification, 10 were further profiled with Western blot, 3 were used for DLS validation, and 1 for Nanostring profiling. Of the 10 samples analyzed by Western blot, 4 were also used for Nanostring analysis, 3 for DLS validation, and 1 for proteomics. Finally, 1 of the 11 Nanostring samples was also used for proteomics. The number of samples processed by each technique is summarized as a **Supplementary Figure S1** online.

Exosome Quantification

Exosomes were isolated from middle ear effusion or human serum (0.5 ml) as a control. The exosome pellets were resuspended and protein concentration measured. The exosomes were gently lysed as to preserve the enzymatic activity of the exosomal AChE enzyme. Exosomes were detected in 13 of the 16 tested MEE samples, and contained between 0.57×10^8 and 33.14×10^8 exosomes. The average quantity of exosomes in these 13 samples was 15.04×10^8 exosomes (**Table 1**).

Table 1. Purified exosome quantification in human MEE samples

MEE sample	Exosome quantity (×108)
1	28.31
2	32.26
3	0
4	1.69
5	0.57
6	6.83
7	0
8	0
9	6.05
10	12.2
11	14.46
12	20.21
13	4.36
14	21.37
15	18.79
16	33.14

MEE, middle ear effusion.

Validation of Purified MEE Exosomes

As an initial strategy, immunoblotting for HSP70, a marker known to be accumulated in body fluid exosomes (32,33), was used to validate purified exosomes. Western blot analyses demonstrated the presence of HSP70 in 8 of 10 samples tested (**Figure 1a**). Importantly, we did not identify CD63 in the purified exosomes. Analysis of eluted exosomal size was performed by DLS of 7 MEEs samples and 1 serum sample. **Figure 1b** shows a DLS curve for a representative sample (MEE 2). This graph shows a distribution of vesicle size across samples between 10 and 300 nm. Overall the mean size of exosomes across samples was 223.02 nm (SD 79.7), with a mean polydispersity index of 0.78 (SD 0.2), signifying a broad diversity in the size distribution of exosomal vesicles **Table 2**). The mean Zeta potential across sample was −9.16 (SD −2.56) indicating the expected presence of negative charged particles.

Transition electron microscopy (TEM) of the isolated vesicles was then performed in order to visually confirm the presence of exosomes. Images revealed vesicular structures ranging from 10–100 nm in size with a central depression gray appearing area for the bigger ones, which is characteristic of TEM imaging of exosomes (34) (**Figure 2a**). Additionally, these vesicular structures were frequently found to aggregate or be involved with entangled filamentous structures, possibly consistent with mucin glycoproteins as reported by others (35) (**Figure 2b**).

Identification of miRNAs in MEE Exosomes

Using then Agilent Small RNA kit and the Agilent RNA 6000 Nano Kit for quality control we identified miRNAs in 10 of 11 samples used for miRNA profiling. There was a mean concentration of 3,835.8 pg/ul miRNA in the samples (range 291.1–21,495.3 pg/μl), with a mean percentage of miRNA purity of 44.5% (range 17–95%) These quality data are summarized in **Table 3**. Out of 800 miRNA nucleotide sequences probed on

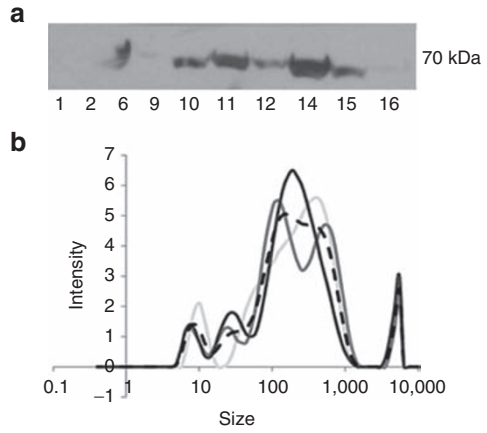

Figure 1. Validation of purified exosomal preparation. (**a**) HSP70 Western Blot analysis of middle ear effusion (MEE). Ten microliters of MEE exsomal eluent were loaded in a polyacrylamide gel before electrophoresis. Proteins were transferred on a nitrocellulose membrane and exposed to specific antibodies to reveal HSP-70. (**b**) Dynamic light scattering (DLS) of three average runs for a representative sample. The size distribution is depicted as the intensity of detection in function of the particle size displayed over a logarithmic scale. Each solid line represents an individual run for a sample. The dashed line represents the average of three runs for one sample.

Table 2. DLS results for purified MEE exosomes

Sample	Average size (nm)	PdI	Zeta potential (mV)
Blood	60.8	0.7	−6.22
2	113.9	0.896	−12.5
3	331.6	0.727	−4.59
5	292.1	0.49	−9.11
7	156.2	1	−7.4
8	299.4	0.491	−9.34
10	147.5	0.93	−10.4
14	220.5	0.9191	−10.8

the Nanostring chip, we identified 29 miRNAs to have relative abundance levels over background, with 17 being unique to MEE over serum controls (as shown in **Figure 3**). Of these, the most abundant miRNA across effusion samples was miR-223-3p, followed by miR-451a, miR-16-2p, miR-320e, and miR-25-3p. PCR was used to validate the presence of miRNAs of interest (miR-223-3p, miR-320e, and miR-16-2p) in extracted exosomes from eight middle ear samples also profiled by Nanostring (**Figure 4**). All the samples tested except the MEE13 were positive for these miRNAs. It is likely there had been RNA degradation in MEE13, explaining the lack of validation. The negative controls blood and nontemplate control (NTC) did not show any signal as expected. Ingenuity Pathway Analysis (IPA) (QIAGEN, Redwood City, CA) was then used to predict the mRNAs targeted by these 17 MEE miRNAs. IPA predicted the regulation of 442 target genes, and among them, genes that dramatically upregulate a large host of IL-8 mediated cellular processes including neutrophil

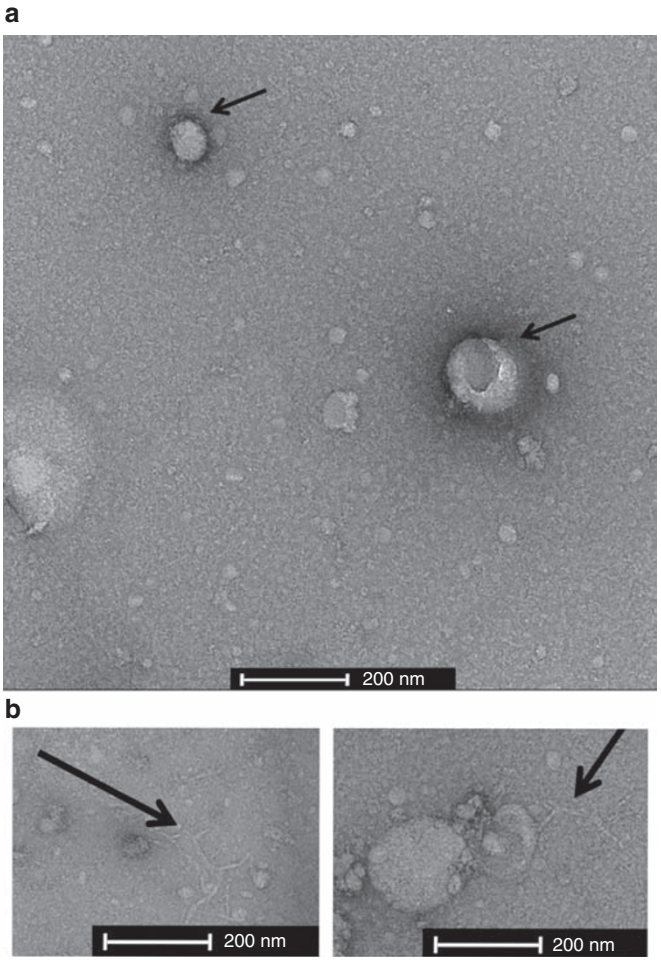

Figure 2. Microscopic analysis of middle ear effusions. (**a** and **b**) TEM of eluted exosomes. Electron microscopy revealed copious amounts of vesicular structures mostly ranging from 10 to 100 nm in size. (**a**) Black arrow points to a larger exosome like structure (about 150 nm), with a characteristic central depression area. (**b**) Black arrows demonstrate entangled filamentous structures involved with the exosome like vesicles, which often appear to be aggregated.

Table 3. Small RNA quality analysis

MEE sample	(miRNA) pg/ul	% miRNA
Blood	615	31
6	291.1	25
9	718.2	24
18	1,043.8	32
19	1,034.3	17
20	701.6	46
21	2,215.3	35
13	21,495.3	82
22	1,415.2	32
14	773.2	57
15	8,670.1	95
16	ND	ND

MEE, middle ear effusion; ND, not determined.

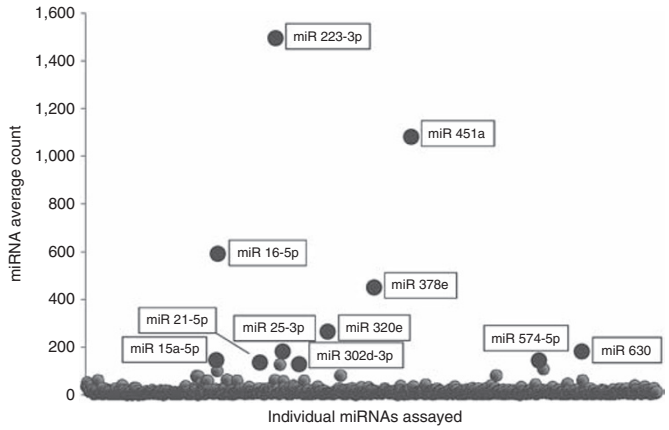

Figure 3. Scatterplot of miRNA abundance within middle ear effusion exosomes. The graph shows the miRNAs assayed by the Nanostring method as average counts. Twenty-nine miRNAs were found to be significantly detected above background. Each dot represents an individual mRNA sequence assayed on the Nanostring chip.

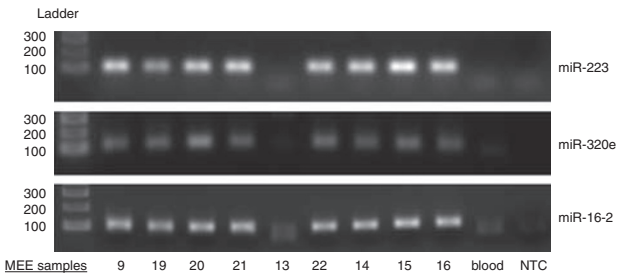

Figure 4. Polymerase chain reaction (PCR) validation of miRNAs of interest. miR-223-3p, miR-320e, and miR-16-2p were validated by RT-qPCR in extracted exosomes from eight independent middle ear samples. The sample number is listed at the bottom. Blood and nontemplate controls (NTC) were also tested for the presence of these microRNAs, considered as negative controls. The middle ear effusion 13 was the only sample that failed to amplify the selected miRNAs.

degranulation (**Figure 5a**), CXCR1/2 mediated signaling associated with antimicrobial defense, lymphocyte and monocyte chemoattraction as well as neutrophil degranulation (**Figure 5b**) and NF-kB proinflammatory upregulation leading to angiogenesis and inflammation (**Figure 5c**).

Proteomic Analysis of Extracted Exosomes

As exosomal vesicles are known to contain proteins which can help elucidate the cellular origin of these, we aimed to profile the protein content of MEE exosomes. For this, we profiled the proteome from 3 MEE using LC-MS/MS. 445 unique proteins were detected (**Supplementary Data** online, **Supplementary Table S1** online) and among them, 29 were found to be specific to MEE exosomes relative to to blood exosomes (**Table 4**). Identified proteins of note appeared to be key regulators of innate immunity including immunoglobulins, mucin MUC5B, heat shock proteins, and BPI fold-containing family B member 1 (BPIFB1); along with typical neutrophil mediators such as myeloperoxidase and neutrophil elastase. IPA was then used to analyze the relationships between the proteins of the MEE exosome proteomic dataset (**Table 5**). Notably, the predominant processes predicted from these group of mediators included glycolysis and hypoxia signaling (P = 2.39E−06 and 4.41E−05, respectively), likely representing responses to the relatively low oxygen environment often cited in the middle ear space of patients with COM. Predicted upstream regulators of the identified proteins included the hypoxia inducible factor-1α (HIF1α) and lipopolysaccharide (P = 3.35E−08 and 7.95E−08, respectively), both notable for being purported mediators of chronic inflammation in the middle ear. Not surprisingly, the top disease and disorders category grouping the identified proteome was diseases associated with an inflammatory response, underlying the chronic inflammatory state in the middle ear during COM.

DISCUSSION

As endocytic vesicles transporting miRNA, proteins, and mRNAs exosomes are described as putative mediators of intercellular communication, we hypothesized that they would be present in middle ear effusion samples and that they would play a role in the pathogenesis of OM. This study for the first time indeed demonstrates that exosomes are present in the MEE of pediatric patients and reports the abundant miRNAs contained within these exosomes. Furthermore, the protein content of these vesicles is also described. Of particular relevance, the identified miRNAs from MEE were found to predictably upregulate transcripts of mediators related to IL-8 activity. As an example, miR-223-b was found to be the most abundant miRNA within MEE exosomes. This miRNA has long been shown to primarily function as a regulator of neutrophil biology. In mice, miR-223 regulates protease activity, neutrophil maturation, and differentiation, modulation of chemotaxis, and granule secretion (36). All of these processes are known to be important during NETosis and miR-223 has been proposed as a regulator of this innate immune response (37). Interestingly, we have recently reported that NETs are a significant component of COM (9). The origin of the exosomes identified in MEE is unclear, and should be the subject of further exploration. It is known that CD15-positive cells such as neutrophils and eosinophils are able to secrete miR-223-b, along with other miRNAs identified herein such as miR-21, miR-142, and miR-338 (28). As such, it is possible that the purified MEE exosomes were in part released by neutrophils (among other immune cells). The nature of the more abundant miRNAs present within MEE exosomes is therefore in line with the premise that infant COM denotes a primarily neutrophilic immune response. Indeed previous work from our group has reported that IL-8 is the most abundant cytokine detected by multiplex assay in MEE samples (9). IL-8 a well-known chemoattractant for neutrophils, and its presence has been shown to positively correlate with the abundance of NETs in bronchial fluids (38). The proteomic profile of MEE derived exosomes also indicate a potential neutrophilic source for their origin, as a large component of the identified mediators are known to be derived from neutrophil granulocytes. Not surprisingly, the top putative pathways from the proteomic list are related

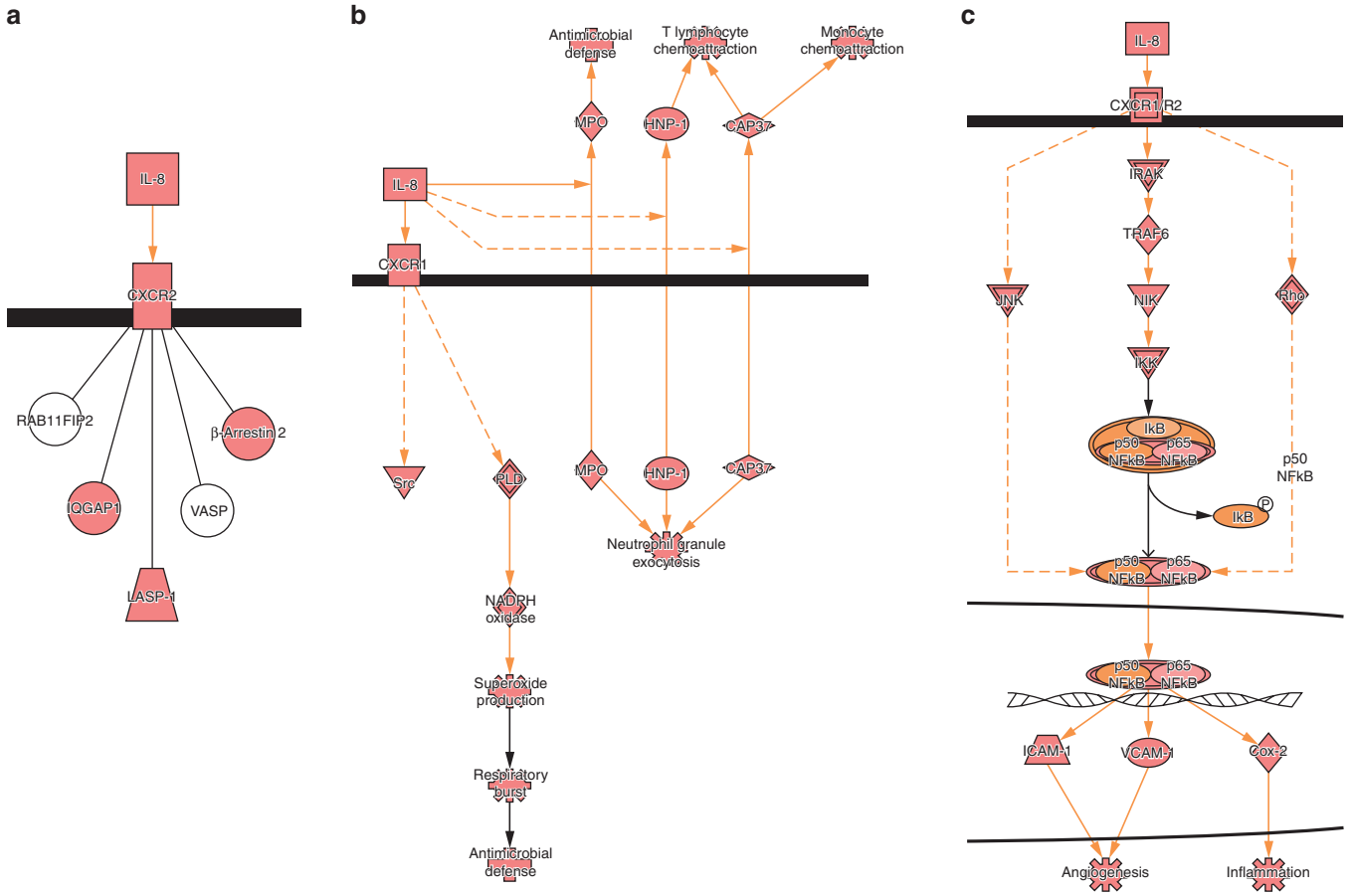

Figure 5. IPA predicted pathways derived from MEE miRNA putative activity. Among the pathways predicted to be regulated by the 17 miRNAs abundant in MEE, IL-8 derived processes were found to predominate, with downstream neutrophil degranulation (**a**), CXCR1-mediated signaling (**b**), and NF-kB proinflammatory upregulation (**c**). The red colored molecules are predicted to be upregulated at the mRNA level by miRNAs, where the orange color is post-translational activation. The solid arrows represent direct activation, and the dotted arrows indirect activation. IL8, interleukin 8; CXCR1, chemokine receptor type 1; MPO, myeloperoxidase; HNP1, defensin alpha 1; PLD, phospholipase D; CAP37, cationic antimicrobial protein/azurocidin; JNK, cJun N-terminal kinase 1; IRAK, interleukin-1 receptor-associated kinase 1; TRAF6, TNF receptor-associated factor 6; NIK, NK-κB-inducing kinase; IKK, IκB-kinase; ICAM1, intercellular adhesion molecule 1; VCAM1, vascular cell adhesion protein 1; Cox2, cycloxygenase 2.

to inflammatory processes. In addition, it is interesting to note the presence of the mucin MUC5B in the exosome proteome. It is possible that MUC5B binds the surface of exosomes, as has been suggested by others (35). This binding may allow for the protein to remain intact during the process of exosome isolation. It is therefore possible that some of the proteins detected in our analysis would bind to the surface of exosomes, rather than being contained within the exosome itself, increasing their putative size.

We believe that some of the other miRNAs detected in MEEs were produced by the middle ear epithelium. In order to analyze this, we have completed a preliminary assay for exosomes in human middle ear epithelial cells (HMEEC) secretions after stimulation with nontypeable *Haemophylus influenzae*. Among the miRNAs detected in HMEEC secretions, 21 were found to also be present in MEE exosomes (data not shown). The eight miRNAs not also detected in HMEEC secreted exosomes include miR-223 (which goes along with our assumption that this miRNA is being secreted into MEE by immune cells such as neutrophils), miR-451a, miR-579, miR-142-3p, miR-144-3p, miR-631, miR-10a-5p, and miR-2682-5p. This underscores the complexity OM pathogenesis and the implication of multiple cell types capable of secreting miRNAs targeting genes in a wide array of cells.

Validation of MEE exosomal size for this study was important as previous reports suggested variability in exosome isolation efficiency (39). To analyze this, we employed DLS and TEM. DLS revealed a mean size of 223.5 nm for the purified exosomes across samples. Although on the surface this may appear as larger than what is typical of exosomes (100 nm), it is in line with what has been reported from respiratory derived exosomes. Using a combination of light scattering techniques, including dynamic light scattering (DLS), Kesimer *et al.* (35) characterized extracellular vesicles derived from the apical secretions of two different cultured airway epithelial cells. The results indicated that epithelial cells release vesicles with a hydrodynamic radius of approximately 340 nm. This larger size was found to be due to the fact that the vesicles were shown to carry filamentous, entangled membrane mucins on their surface that increases their overall radius. As mentioned our

Table 4. Middle ear effusion proteins identified by LC-MS/MS

Accession	Description	Total peptide counts
P01833	Polymeric immunoglobulin receptor (PIGR)	105
O43707	Alpha-actinin-4 (ACTN4)	90
P26038	Moesin (MSN)	85
Q8TDL5	BPI fold-containing family B member 1 (BPIFB1)	75
P01602	Ig kappa chain V-I region HK102 (Fragment) (IGKV1-5)	71
P05164	Myeloperoxidase (MPO)	70
P01596	Ig kappa chain V-I region CAR	66
P14618	Pyruvate kinase isozymes M1/M2 (PKM)	65
P07900	Heat shock protein HSP 90-alpha (HSP90AA1)	62
P01593	Ig kappa chain V-I region AG	58
P13796	Plastin-2 (LCP1)	54
P08238	Heat shock protein HSP 90-beta (HSP90AB1)	52
P01743	Ig heavy chain V-I region HG3	46
P31146	Coronin-1A (CORO1A)	43
P29401	Transketolase (TKT)	41
O15144	Actin-related protein 2/3 complex subunit 2 (ARPC2)	29
P46940	Ras GTPase-activating-like protein IQGAP1 (IQGAP1)	27
P06733	Alpha-enolase (ENO1)	25
P80723	Brain acid soluble protein 1 (BASP1)	25
P06744	Glucose-6-phosphate isomerase (GPI)	24
P04217	Alpha-1B-glycoprotein (A1BG)	22
P62805	Histone H4 (HIST1H4A)	22
P01700	Ig lambda chain V-I region HA	20
P01019	Angiotensinogen (AGT)	19
Q9HC84	Mucin-5B (MUC5B)	19
P00338	L-lactate dehydrogenase A chain (LDHA)	18
P08246	Neutrophil elastase (ELANE)	18
P24158	Myeloblastin (PRTN3)	17
P06331	Ig heavy chain V-II region ARH-77	13

Table 5. Pathway analysis of the middle ear effusion exosome proteomic dataset

Top canonical pathways	*P* value	Overlap %
Glycolysis	2.39E−06	12
Hypoxia signaling	4.41E−05	4.6
Remodeling of epithelial junctions	5.05E−05	4.4
Actin cytoskeleton signaling	7.38E−05	1.9
Upstream regulators	*P* value	
HIF1α	3.35E−08	
LPS	7.93E−08	
Diseases and disorders	*P* value	Molecules
Inflammatory response	5.32E−03 to 1.62E−06	15
Molecular and cellular functions	*P* value	Molecules
Cellular movement	6.07E−03 to 3.24E−12	18
Cellular function and maintenance	5.32E−03 to 3.52E−08	17
Cell-to-cell signaling and interaction	6.38E−03 to 2.12E−07	13
Cell death and survival	6.38E−03 to 3.16E−07	17
Cellular assembly and organization	4.95E−03 to 1.37E−06	11

LPS, lipopolysaccharide.

proteomic analysis revealed mucin MUC5B to be abundant, and its presence is a potential explanation for the larger size of the MEE-derived exosomes. Moreover, TEM imaging of the isolated vesicles demonstrated a broad distribution of vesicular size along with frequent aggregation of these. Filamentous protein-like structures were also noted associated with the vesicles, similar to what was reported by Kesimer *et al.* in exosomes isolated from airway epithelium (35).

The global analysis of MEE exosomal miRNAs and proteins using IPA confirmed the importance of middle ear inflammation during COM, and the implication of IL-8 related responses (13,40). This finding is in line with our recent report of NETs predominance in COM effusions. IPA also predicted glycolysis pathway activation, a finding likely representing upregulated metabolic activity in the samples. It is also relevant to find that IPA predicted upregulation of hypoxia pathways, as previous animal and *in vitro* studies have suggested hypoxia to be a common pathophysiologic condition of COM (41,42). In future studies, we hope to investigate the role of identified miRNAs in the OM pathogenesis, especially miR-223, the most abundant miRNA in MEE exosomes.

Our report is limited though by the fact that our characterization of exosomes in middle ear fluids only represents a "snapshot" in time, which may vary quite a bit during OM progression over time. Also, given sample limitations, it was not possible to assay every sample by each experimental technique. Another limitation to our study was the fact that we did not identify CD63 by western blot in the purified exosomes. Although CD63 is a broadly used exosomal marker, but it is worthy to note that it may become undetectable in biospecimens containing relatively low amounts of exsosomes. Indeed, others have called into question the use of CD63 as a standard exosomal marker since the expression level of this tetraspanin is often considerably lower than other markers (43).

Conclusion

This is to our knowledge the first report demonstrating the presence of exosomes transporting miRNAs in MEEs. Abundant miRNAs and proteins in these exosomes appear to be critical mediators of innate immunity and neutrophilia. These findings open a broad and novel area of research in OM pathophysiology as driven by miRNA cell communication.

SUPPLEMENTARY MATERIAL

Supplementary material is linked to the online version of the paper at http://www.nature.com/pr

ACKNOWLEDGMENTS

The electron microscopy analysis was carried out at the GWNIC (George Washington University Nanofabrication and Imaging Center) with the help of Christine Brantner and Anastas Popratiloff.

STATEMENT OF FINANCIAL SUPPORT

This work was supported by R01DC012377 from the NIDCD and also partially supported by NIH core grants 2R24HD050846-06 (National Center for Medical Rehabilitation Research), NICHD 5P30HD040677 (Intellectual and Developmental Disabilities Research Center), and UL1TR000075 (NIH National Center for Advancing Translational Sciences). Its contents are solely the responsibility of the authors and do not necessarily represent the official views of the National Center for Advancing Translational Sciences or the National Institutes of Health.

Disclosure: None to report.

REFERENCES

1. Cherry DK, Woodwell DA. National ambulatory medical care survey: 2000 summary. Adv Data. 2002 Jun 5;(328):1–32.
2. Grubb MS, Spaugh DC. Treatment failure, recurrence, and antibiotic prescription rates for different acute otitis media treatment methods. Clin Pediatr (Phila) 2010;49:970–5.
3. Ahmed S, Shapiro NL, Bhattacharyya N. Incremental health care utilization and costs for acute otitis media in children. Laryngoscope 2014;124:301–5.
4. Rosenfeld RM, Casselbrant ML, Hannley MT. Implications of the AHRQ evidence report on acute otitis media. Otolaryngol Head Neck Surg 2001;125:440–8; discussion 439.
5. Lim DJ, Birck H. Ultrastructural pathology of the middle ear mucosa in serous otitis media. Ann Otol Rhinol Laryngol 1971;80:838–53.
6. Tos M, Bak-Pedersen K. Goblet cell population in the pathological middle ear and eustachian tube of children and adults. Ann Otol Rhinol Laryngol 1977;86(2 pt. 1):209–18.
7. Ryan AF, Jung TT, Juhn SK, et al. Recent advances in otitis media. 4A. Molecular biology. Ann Otol Rhinol Laryngol Suppl 2005;194:42–9.
8. Hurst DS, Venge P. The impact of atopy on neutrophil activity in middle ear effusion from children and adults with chronic otitis media. Arch Otolaryngol Head Neck Surg 2002;128:561–6.
9. Val S, Poley M, Brown K, et al. Proteomic characterization of middle ear fluid confirms neutrophil extracellular traps as a predominant innate immune response in chronic otitis media. PLoS One 2016;11:e0152865.
10. King LB, Pang B, Perez AC, et al. Observation of Viable Nontypeable *Haemophilus Influenzae* Bacteria within Neutrophil Extracellular Traps in Clinical Samples from Chronic Otitis Media. Otolaryngology 2013;3:145. doi: 10.4172/2161-119X.1000145.
11. Thornton RB, Wiertsema SP, Kirkham LA, et al. Neutrophil extracellular traps and bacterial biofilms in middle ear effusion of children with recurrent acute otitis media–a potential treatment target. PLoS One 2013;8:e53837.
12. Preciado D, Goyal S, Rahimi M, et al. MUC5B is the predominant mucin glycoprotein in chronic otitis media fluid. Pediatr Res 2010;68:231–6.
13. Val S. "Basic Science Concepts in Otitis Media Pathophysiology and Immunity" In: Otitis Media State of the Art Concepts and Treatment. Preciado D, ed. Springer International Publishing: Gewerbestrasse Switzerland. 2015:53–79.
14. Sadé J, Fuchs C. Secretory otitis media in adults: I. The role of mastoid pneumatizationas a risk factor. Ann Otol Rhinol Laryngol 1996;105:643–7.
15. Lin J, Tsuprun V, Kawano H, et al. Characterization of mucins in human middle ear and Eustachian tube. Am J Physiol Lung Cell Mol Physiol 2001;280:L1157–67.
16. Lin J, Tsuboi Y, Rimell F, et al. Expression of mucins in mucoid otitis media. J Assoc Res Otolaryngol 2003;4:384–93.
17. Camussi G, Deregibus MC, Bruno S, Grange C, Fonsato V, Tetta C. Exosome/microvesicle-mediated epigenetic reprogramming of cells. Am J Cancer Res 2011;1:98–110.
18. Ferrante SC, Nadler EP, Pillai DK, et al. Adipocyte-derived exosomal miRNAs: a novel mechanism for obesity-related disease. Pediatr Res 2015;77:447–54.
19. Bartel DP. MicroRNAs: target recognition and regulatory functions. Cell 2009;136:215–33.
20. Camussi G, Deregibus MC, Bruno S, Cantaluppi V, Biancone L. Exosomes/microvesicles as a mechanism of cell-to-cell communication. Kidney Int 2010;78:838–48.
21. O'Neill LA, Sheedy FJ, McCoy CE. MicroRNAs: the fine-tuners of Toll-like receptor signalling. Nat Rev Immunol 2011;11:163–75.
22. Ardekani AM, Naeini MM. The role of microRNAs in human diseases. Avicenna J Med Biotechnol 2010;2:161–79.
23. Kim YK. Extracellular microRNAs as biomarkers in human disease. Chonnam Med J 2015;51:51–7.
24. Song JJ, Kwon SK, Cho CG, Park SW, Chae SW. Microarray analysis of microRNA expression in LPS induced inflammation of human middle ear epithelial cells (HMEECs). Int J Pediatr Otorhinolaryngol 2011;75:648–51.
25. Moon HG, Cao Y, Yang J, Lee JH, Choi HS, Jin Y. Lung epithelial cell-derived extracellular vesicles activate macrophage-mediated inflammatory responses via ROCK1 pathway. Cell Death Dis 2015;6:e2016.
26. Lee H, Zhang D, Minhas J, Jin Y. Extracellular Vesicles Facilitate the Intercellular Communications in the Pathogenesis of Lung Injury. Cell Dev Biol. 2016;5:1-7. pii: 175.
27. Val S, Burgett K, Brown KJ, Preciado D. SuperSILAC quantitative proteome profiling of murine middle ear epithelial cell remodeling with NTHi. PLoS One 2016;11:e0148612.
28. Leidinger P, Backes C, Dahmke IN, et al. What makes a blood cell based miRNA expression pattern disease specific?–a miRNome analysis of blood cell subsets in lung cancer patients and healthy controls. Oncotarget 2014;5:9484–97.
29. Tian C, Li Z, Yang Z, Huang Q, Liu J, Hong B. Plasma microRNA-16 is a biomarker for diagnosis, stratification, and prognosis of hyperacute cerebral infarction. PLoS One 2016;11:e0166688.
30. Preciado D, Poley M, Tsai S, Tomney A, Brown K, Val S. A proteomic characterization of NTHi lysates. Int J Pediatr Otorhinolaryngol. 2016 Jan;80:8-16. doi: 10.1016/j.ijporl.2015.11.016. PubMed PMID: 26746604; PubMed Central PMCID: PMC4706994.
31. Saieg A, Brown KJ, Pena MT, Rose MC, Preciado D. Proteomic analysis of pediatric sinonasal secretions shows increased MUC5B mucin in CRS. Pediatr Res 2015;77:356–62.
32. Lässer C, Alikhani VS, Ekström K, et al. Human saliva, plasma and breast milk exosomes contain RNA: uptake by macrophages. J Transl Med 2011;9:9.
33. Keller S, Ridinger J, Rupp AK, Janssen JW, Altevogt P. Body fluid derived exosomes as a novel template for clinical diagnostics. J Transl Med 2011;9:86.
34. Wu Y, Deng W, Klinke DJ 2nd. Exosomes: improved methods to characterize their morphology, RNA content, and surface protein biomarkers. Analyst 2015;140:6631–42.
35. Kesimer M, Gupta R. Physical characterization and profiling of airway epithelial derived exosomes using light scattering. Methods 2015;87:59–63.
36. Gantier MP. The not-so-neutral role of microRNAs in neutrophil biology. J Leukoc Biol 2013;94:575–83.
37. Baek D, Villén J, Shin C, Camargo FD, Gygi SP, Bartel DP. The impact of microRNAs on protein output. Nature 2008;455:64–71.
38. Hamaguchi S, Hirose T, Matsumoto N, et al. Neutrophil extracellular traps in bronchial aspirates: a quantitative analysis. Eur Respir J 2014;43:1709–18.
39. Petersen KE, Manangon E, Hood JL, et al. A review of exosome separation techniques and characterization of B16-F10 mouse melanoma exosomes with AF4-UV-MALS-DLS-TEM. Anal Bioanal Chem 2014;406:7855–66.
40. Hirano T, Kodama S, Kawano T, Suzuki M. Accumulation of regulatory T cells and chronic inflammation in the middle ear in a mouse model of chronic otitis media with effusion induced by combined eustachian tube blockage and nontypeable haemophilus influenzae infection. Infect Immun 2015;84:356–64.
41. Huang Q, Zhang Z, Zheng Y, et al. Hypoxia-inducible factor and vascular endothelial growth factor pathway for the study of hypoxia in a new model of otitis media with effusion. Audiol Neurootol 2012;17:349–56.
42. Bhutta MF, Cheeseman MT, Brown SD. Myringotomy in the Junbo mouse model of chronic otitis media alleviates inflammation and cellular hypoxia. Laryngoscope 2014;124:E377–83.
43. Jørgensen M, Bæk R, Pedersen S, Søndergaard EK, Kristensen SR, Varming K. Extracellular Vesicle (EV) Array: microarray capturing of exosomes and other extracellular vesicles for multiplexed phenotyping. J Extracell Vesicles. 2013;2. doi: 10.3402/jev.v2i0.20920. PubMed PMID: 24009888; PubMed Central PMCID: PMC3760630.